

Mask Approximation Net: Merging Feature Extraction and Distribution Learning for Remote Sensing Change Captioning

Dongwei Sun, Xiangyong Cao

Abstract—Remote sensing image change description, as a novel multimodal task in the field of remote sensing processing, not only enables the detection of changes in surface conditions but also provides detailed descriptions of these changes, thereby enhancing human interpretability and interactivity. However, previous methods mainly employed Convolutional Neural Network (CNN) architectures to extract bitemporal image features. This approach often leads to an overemphasis on designing specific network architectures and limits the captured feature distributions to the current dataset, resulting in poor generalizability and robustness when applied to other datasets or real-world scenarios. To address these limitations, this paper proposes a novel approach for remote sensing image change detection and description that integrates diffusion models, aiming to shift the focus from conventional feature learning paradigms to data distribution learning. The proposed method primarily includes a simple multi-scale change detection module, whose output features are subsequently refined using a diffusion model. Additionally, we introduce a frequency-guided complex filter module to handle high-frequency noise during the diffusion process, which helps to maintain model performance. Finally, we validate the effectiveness of our proposed method on several remote sensing change detection description datasets, demonstrating its superior performance. The code available at [MaskApproxNet](#)

Index Terms—Remote sensing image, Change Captioning, Diffusion Model.

I. INTRODUCTION

REMOTE sensing change captioning has gained significant attention in recent years due to its ability to provide detailed, natural-language descriptions of temporal variations in the Earth’s surface. Despite this progress, existing methods, predominantly based on Convolutional Neural Networks (CNNs), have several shortcomings that limit their practical applicability. The most notable issue with these traditional methods is their reliance on complex network architectures specifically designed for feature extraction from bitemporal images, which often results in limited generalizability across datasets. Such methods struggle to adapt to different domains, and their effectiveness diminishes when applied to scenarios or datasets that differ significantly from those used during training. Moreover, CNN-based methods are prone to overfitting, making it difficult to ensure robustness and reliability in real-world applications, especially where data distribution varies. These issues significantly restrict the practical use of remote sensing change captioning in diverse and dynamic environments.

To address these limitations, we propose a novel method that leverages diffusion models for remote sensing image change

captioning. Diffusion models, which focus on learning data distributions rather than merely extracting features, provide a powerful alternative that can better capture the complex nature of temporal changes in remote sensing imagery. Our method integrates a multi-scale change captioning module to identify changes at various scales and refines these outputs through a diffusion process, resulting in more robust and adaptive caption generation. By shifting the paradigm from feature-based learning to distribution-based learning, our approach offers significant improvements in generalizability and robustness. Furthermore, we introduce a frequency-guided complex filter module to effectively manage high-frequency noise that can degrade model performance during the diffusion process. This combination ensures that the learned representations are not only accurate but also resilient to noise, enhancing the overall quality of generated captions.

Our approach provides several key advantages over existing methods. First, it enhances the generalizability of change captioning models by focusing on data distribution learning, making it more adaptable to diverse and unseen datasets. Second, the use of a diffusion model enables effective refinement of features, leading to improved caption quality and accuracy. Third, the frequency-guided complex filter module addresses high-frequency noise, thereby maintaining the integrity of the model’s output. Extensive experiments conducted on multiple remote sensing change captioning datasets demonstrate that our proposed method consistently outperforms state-of-the-art approaches in terms of captioning accuracy and robustness. These improvements make our framework highly suitable for real-world applications where interpretability and adaptability are crucial.

In summary, our work introduces a robust and adaptable framework for remote sensing change captioning by integrating diffusion models and a frequency-guided filtering mechanism. The highlights of our proposed method include enhanced generalizability through data distribution learning, refined feature representation via the diffusion model, and effective noise management to preserve output quality. This comprehensive approach ensures that our model not only performs well on standard datasets but also excels in challenging, real-world scenarios. Summary of the contributions of this paper is as follows:

- **Enhanced Generalizability:** Our method improves generalizability through data distribution learning, enabling better adaptation to diverse datasets.
- **Refined Feature Representation:** The diffusion model

enhances feature representation, leading to more accurate and meaningful results.

- **Experimental Validation:** The effectiveness of our method is validated through experiments on standard datasets, demonstrating its robustness and reliability.

The paper is organized as follows: Section II provides a review of related work, while Section III outlines the proposed method in detail. Section IV presents the experimental setup, including comprehensive descriptions and an analysis of the results. The article concludes with a brief summary in Section V.

II. RELATED WORK

A. Change Captioning

The RSICC task has garnered significant attention in recent years due to its capability to describe differences between bitemporal remote sensing (RS) images using natural language. Hoxha et al. [1] introduced early and late feature fusion strategies to integrate bitemporal visual features, utilizing an RNN and a multiclass SVM decoder for generating change captions. Chouaf et al. [2] were among the first to explore the RSICC task, employing a CNN as a visual encoder to capture temporal scene changes and an RNN as a decoder to produce descriptive change captions.

Transformer networks [3], incorporating the multi-head attention (MHA) mechanism, have gained prominence in image analysis and achieved notable success in image change captioning. Liu et al. [4] advanced the field by proposing a transformer-based encoder-decoder framework for RSICC. Their method includes a dual-branch transformer encoder for detecting scene changes and a multistage fusion module for combining multilayer features to generate change descriptions. Subsequently, Liu et al. [5] refined their approach by introducing progressive difference perception transformer layers, which effectively capture both high-level and low-level semantic changes. Furthermore, Liu et al. [6] proposed a prompt-based strategy that leverages pretrained large language models (LLMs) for RSICC tasks, using visual features, change classes, and language representations as prompts for a frozen LLM to generate change captions. Chang [7] developed an attentive network for RS change captioning, named Chg2Cap, which harnesses the strengths of transformer models commonly used in NLP. [8] proposes a lightweight Sparse Focus Transformer for remote sensing image change captioning, which significantly reduces parameters and computational complexity while maintaining competitive performance. DiffusionRSCC [9] introduced an innovative diffusion model (Diffusion-RSCC) for RSICC, employing a forward noising and reverse denoising process to learn the probabilistic distribution of the input. SEN [10] proposed a bitemporal pretraining method that leverages self-supervised learning on a large-scale bitemporal RS image dataset. This approach reduces data distribution and input gaps, resulting in more suitable features for RSICC and improved model generalization.

B. Generative Models

Generative Adversarial Networks (GANs), as a typical generative approach, are widely used in the field of remote

sensing imagery, particularly in change detection. [11] this research introduces a Dual Attentive Generative Adversarial Network (DAGAN) for high-resolution remote sensing image change detection. By designing a multi-level feature extractor and a multi-scale adaptive fusion module, DAGAN effectively integrates features at various levels, enhancing the accuracy of change detection. CD-GAN[12] presents an unsupervised change detection method named CD-GAN, tailored for heterogeneous remote sensing images acquired from different sensors. By integrating generative adversarial networks, CD-GAN can detect change regions without the need for image registration, improving robustness and accuracy. By generating better-registered images through GANs, [13] the method mitigates the impact of misregistration on change detection, thereby enhancing detection performance.

Within the enormous models for CD, DDPM-based architectures emerge with distinguished advantages over traditional CNNs and transformers. DDPM-CD [14] by pre-training the DDPM on a large set of unlabeled remote sensing images, multi-scale feature representations are obtained. A lightweight change detection classifier is then fine-tuned to detect precise changes. [15] designed to guide the generation of change detection maps by exploiting multi-level difference features. The Similar ideas have also applied in medicine field. The model [9] employs a noise predictor conditioned on cross-modal features to generate human-like descriptions of semantic changes between bi-temporal remote sensing image pairs. The authors [16] propose dynamic conditional encoding to enhance step-wise regional attention and a Feature Frequency Parser (FF-Parser) to mitigate high-frequency noise for medical image segmentation. [17] presents a graph attention-guided diffusion model tailored for liver vessel segmentation. By integrating graph attention mechanisms with diffusion probabilistic models, the approach effectively captures complex vascular structures in liver images.

III. METHOD

In this section, we propose a novel diffusion model-based approach for the remote sensing image change captioning task, leveraging mask generation for change captioning. The proposed method consists of two key phases: 1) Mask Approximation Phase, and 2) Text Decoder Decoding Phase. The primary objective of the first phase is to construct a mapping from the change distribution to the standard Gaussian distribution by utilizing the designed MaskApproxNet network, which extracts change features from the pre-change image and post-change image. In the reverse denoising process, the prior mask is transformed from the standard Gaussian distribution back to the real data distribution using a denoiser network.

In the following parts, we will first introduce the core concept of diffusion models using DDPM as an example. Then, we will provide a detailed explanation of the entire implementation process in the Mask Approximation Phase, including the detailed design of MaskApproxNet and the Frequency Noise Filter. Finally, we will focus on the Text Decoder process.

A. Denoising Diffusion Models

Diffusion models operate by defining a forward Markov process that gradually transforms data into noise and a reverse process that reconstructs data from noise. Formally, given an initial data distribution $\mathbf{x}_0 \sim q(\mathbf{x}_0)$, the forward process generates a sequence of variables $\mathbf{x}_1, \mathbf{x}_2, \dots, \mathbf{x}_T$ using a transition kernel $q(\mathbf{x}_t | \mathbf{x}_{t-1})$. By applying the Markov property and the chain rule, the joint distribution of the sequence conditioned on \mathbf{x}_0 can be expressed as:

$$q(\mathbf{x}_1, \dots, \mathbf{x}_T | \mathbf{x}_0) = \prod_{t=1}^T q(\mathbf{x}_t | \mathbf{x}_{t-1}). \quad (1)$$

In the context of denoising diffusion probabilistic models (DDPMs), the transition kernel $q(\mathbf{x}_t | \mathbf{x}_{t-1})$ is designed to gradually transform the data distribution $q(\mathbf{x}_0)$ into a simple, tractable prior. A common choice for this kernel is a Gaussian perturbation, defined as:

$$q(\mathbf{x}_t | \mathbf{x}_{t-1}) = \mathcal{N}(\mathbf{x}_t; \sqrt{1 - \beta_t} \mathbf{x}_{t-1}, \beta_t \mathbf{I}), \quad (2)$$

where $\beta_t \in (0, 1)$ is a predefined hyperparameter. This Gaussian kernel allows the joint distribution to be marginalized analytically, yielding:

$$q(\mathbf{x}_t | \mathbf{x}_0) = \mathcal{N}(\mathbf{x}_t; \sqrt{\bar{\alpha}_t} \mathbf{x}_0, (1 - \bar{\alpha}_t) \mathbf{I}), \quad (3)$$

where $\alpha_t = 1 - \beta_t$ and $\bar{\alpha}_t = \prod_{s=0}^t \alpha_s$. A sample \mathbf{x}_t can then be generated from \mathbf{x}_0 using the transformation:

$$\mathbf{x}_t = \sqrt{\bar{\alpha}_t} \mathbf{x}_0 + \sqrt{1 - \bar{\alpha}_t} \boldsymbol{\epsilon}, \quad (4)$$

where $\boldsymbol{\epsilon} \sim \mathcal{N}(\mathbf{0}, \mathbf{I})$. When $\bar{\alpha}_T \approx 0$, the final state \mathbf{x}_T approximates a Gaussian distribution, $q(\mathbf{x}_T) \approx \mathcal{N}(\mathbf{0}, \mathbf{I})$.

Intuitively, the forward process adds noise step by step, erasing data structure until only noise remains. To generate new data, DDPMs reverse this process. Starting with a noise sample $\mathbf{x}_T \sim \mathcal{N}(\mathbf{0}, \mathbf{I})$, the reverse Markov chain iteratively removes noise to reconstruct the data.

The reverse process is parameterized by a prior $p(\mathbf{x}_T) = \mathcal{N}(\mathbf{0}, \mathbf{I})$ and a learnable transition kernel $p_\theta(\mathbf{x}_{t-1} | \mathbf{x}_t)$, which is modeled as:

$$p_\theta(\mathbf{x}_{t-1} | \mathbf{x}_t) = \mathcal{N}(\mathbf{x}_{t-1}; \mu_\theta(\mathbf{x}_t, t), \Sigma_\theta(\mathbf{x}_t, t)), \quad (5)$$

where $\mu_\theta(\mathbf{x}_t, t)$ and $\Sigma_\theta(\mathbf{x}_t, t)$ are neural network outputs parameterized by θ . The reverse chain starts from \mathbf{x}_T and iteratively samples \mathbf{x}_{t-1} until reaching \mathbf{x}_0 , yielding a generated data sample.

B. Mask Approximation Phase

The proposed algorithm model is shown in Figure 1 and is divided into two main stages. The first stage, the **Mask Approximation Phase**, primarily processes the given remote sensing images I_{pre} and I_{post} . It utilizes the designed Mask Approx Module for simple feature processing, combines the results with a Noisy Mask, and sends them to the UNet denoising network to generate change features. These features are then passed to the second stage, the **Text Decoder**, to generate change detection descriptions. Next, we will introduce each of these two stages in detail.

1) *Mask Approx Module*: The proposed framework as illustrated Figure 2, which processes a pair of bi-temporal remote sensing (RS) images, denoted as I_{pre} (pre-change image) and I_{post} (post-change image), through a systematic pipeline. First, a Siamese ResNet backbone is utilized to extract multi-scale features at four levels, represented as X_i^{pre} and X_i^{post} for $i \in \{1, 2, 3, 4\}$, where:

$$X_i^{pre} = \text{ResNet}(I_{pre}, i), \quad X_i^{post} = \text{ResNet}(I_{post}, i).$$

These features are then input to a difference module, which separately processes the multi-scale features and combines them through a convolution layer to generate rich feature encodings, denoted as \bar{X} :

$$\bar{X} = \text{Conv}(\text{DifferenceModule}(X_i^{pre}, X_i^{post})).$$

The encoded representations \bar{X} are passed to a decoder that upsamples the features to match the spatial resolution of the input images. The decoder employs two transpose convolution layers:

$$\bar{X}_{\text{upsampled}} = \text{TransposeConv}(\bar{X}),$$

followed by a residual convolutional block for feature enhancement:

$$\bar{X}_{\text{refined}} = \text{ResidualBlock}(\bar{X}_{\text{upsampled}}).$$

Finally, a convolution layer is applied to the refined features to produce the predicted difference image DiffImage:

$$\text{DiffImage} = \text{Conv}(\bar{X}_{\text{refined}}).$$

This integrated framework effectively extracts, processes, and decodes change representations to achieve accurate change detection.

To achieve denoising, we employ U-Net as the core network. During the forward process, the change label \mathbf{x}_0 undergoes a sequence of T steps where Gaussian noise is progressively added. Conversely, the reverse process is designed to reconstruct the original data by systematically removing the noise. The reverse process is mathematically defined as:

$$p_\theta(\mathbf{x}_{0:T-1} | \mathbf{x}_T) = \prod_{t=1}^T p_\theta(\mathbf{x}_{t-1} | \mathbf{x}_t) \quad (6)$$

where θ denotes the learnable parameters of the reverse process. The initial state of the reverse process starts from a Gaussian noise distribution $p_\theta(\mathbf{x}_T) = \mathcal{N}(\mathbf{x}_T; \mathbf{0}, \mathbf{I}_{n \times n})$, where \mathbf{I} represents the raw input image. Through this iterative reverse process, the latent variable distribution $p_\theta(\mathbf{x}_T)$ transitions to the target data distribution $p_\theta(\mathbf{x}_0)$.

Figure 2 illustrates the conditioning of the reverse process on temporal remote sensing (RS) images. This process is defined as follows:

$$\begin{aligned} \boldsymbol{\epsilon}_\theta(\mathbf{x}_t, I_{pre}, I_{post}, t) = & \text{UNet}(\text{Cat}(I_{pre}, \text{MaskNoise}), \\ & \text{Cat}(I_{post}, \text{MaskNoise}), \\ & \text{Cat}(\text{Diff_image}, \text{MaskNoise}), t) \end{aligned} \quad (7)$$

where $\text{Cat}(\cdot)$ represents the concatenation operation. The variables I_{pre} and I_{post} correspond to the remote sensing images

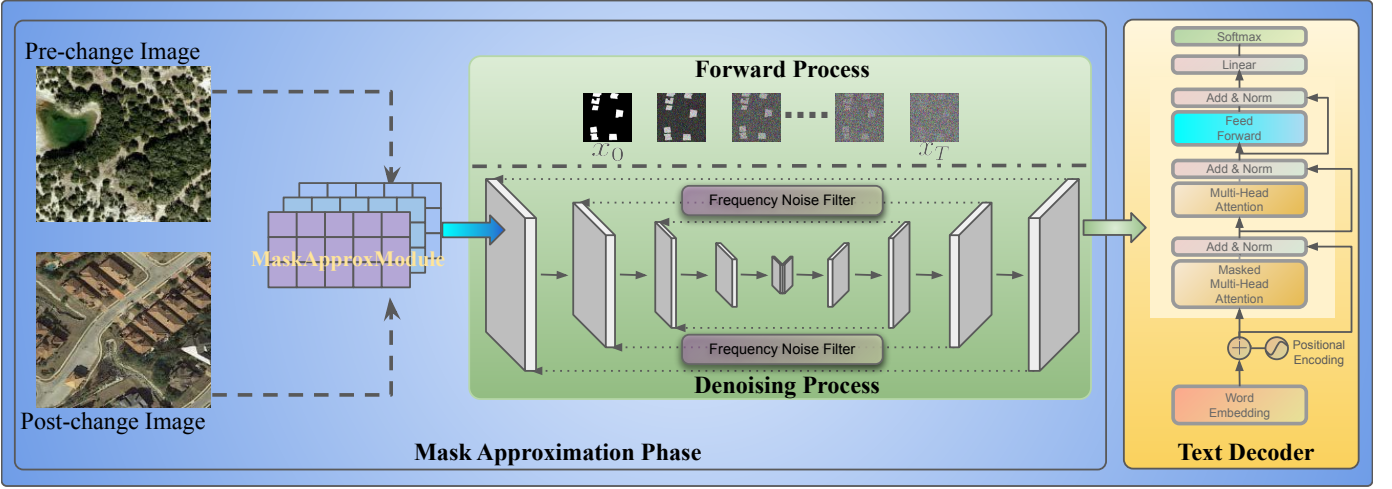


Fig. 1. The flowchart illustrates the overall framework of the proposed algorithm, highlighting its two main stages: the Mask Approximation Phase for feature processing and change feature generation, and the Text Decoder Phase for generating change detection descriptions

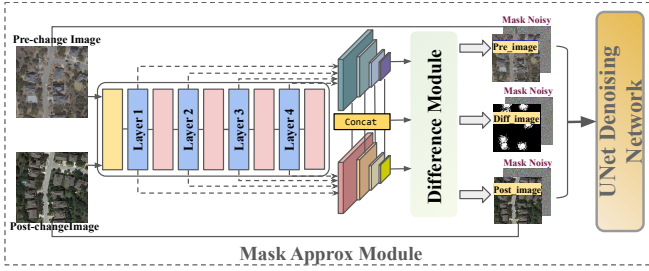


Fig. 2. The flowchart highlights the Mask Approximation Phase, showcasing the process of multi-scale feature extraction, difference computation, and feature refinement to generate a precise difference image for change detection

before and after the event, respectively. Diff_image captures the difference between the two temporal images by Mask Approx Module, while MaskNoise introduces noise to the mask during the denoising process.

The estimated noise is iteratively utilized to guide the sampling process at each step, following the equations (1)-(5). The sampling formula is expressed as:

$$\mathbf{x}_{t-1} = \sqrt{\frac{1}{\alpha_t}} \mathbf{x}_t - \sqrt{\frac{1-\alpha_t}{1-\bar{\alpha}_t}} \epsilon(\mathbf{x}_t, I_{pre}, I_{post}, t) + \tilde{\beta}_t \mathbf{z}, \quad (8)$$

where $\mathbf{z} \sim \mathcal{N}(\mathbf{0}, \mathbf{I}_{n \times n})$ is a random vector with elements sampled independently from a standard normal distribution. After performing iterations of this sampling process [18], change detection (CD) map is generated, starting from Gaussian noise.

2) *Frequency Noise Filter*: Frequency-Guided Channel Fusion (FGCF) is a method designed for noise suppression in high-dimensional data as shown in Figure 3, by leveraging frequency-domain analysis. Let $X \in \mathbb{R}^{C \times H \times W}$ represent the input feature tensor, where C is the number of channels, and H and W are the spatial dimensions. The method starts by transforming each channel of the input tensor into the frequency domain using the Discrete Fourier Transform (DFT), defined as

$$\hat{X}_c = F(X_c)$$

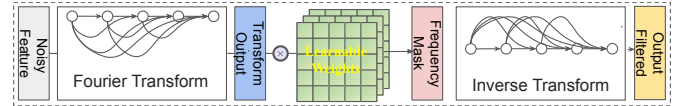


Fig. 3. The flowchart illustrates the overall process of the Frequency-Guided Channel Fusion (FGCF) method, encompassing frequency-domain transformation, frequency-guided weighting, inverse transformation to the spatial domain, and channel-wise attention for feature fusion.

where F denotes the Fourier transform and $\hat{X}_c \in \mathbb{C}^{H \times W}$ is the frequency representation of the c -th channel. To suppress high-frequency noise, a frequency-guided weighting function $W_c(f_x, f_y)$ is applied to each frequency component (f_x, f_y) of \hat{X}_c . The weighting function is defined as

$$W_c(f_x, f_y) = \exp(-\alpha \cdot \|F(f_x, f_y)\|_2^2)$$

where $F(f_x, f_y)$ is a learnable frequency filter and α is a scaling parameter controlling the suppression strength. The filtered frequency representation becomes

$$\hat{X}'_c = W_c \odot \hat{X}_c$$

where \odot denotes element-wise multiplication. After filtering, the frequency-domain representation is transformed back to the spatial domain using the Inverse Fourier Transform (IFT):

$$X'_c = F^{-1}(\hat{X}'_c)$$

To aggregate complementary information across channels, a channel attention mechanism is applied, where the channel-wise attention weights A_c are computed as

$$A_c = \sigma(W_a \cdot \text{GAP}(X'_c) + b_a),$$

with GAP representing Global Average Pooling, W_a and b_a as learnable parameters, and σ as the sigmoid activation function. The final fused feature tensor is obtained by summing the weighted features from all channels:

$$X_{FGCF} = \sum_{c=1}^C A_c \cdot X'_c$$

The advantages of FGCF include frequency-domain adaptation, which targets specific frequency bands to suppress noise more effectively than purely spatial-domain methods, and channel fusion, which enhances the network’s ability to preserve essential features while suppressing noise. The method also ensures parameter efficiency, as the learnable components such as the frequency filter F , the channel attention weights W_a , and the bias b_a are lightweight, introducing minimal computational overhead.

C. Text Decoder Phase

Caption training. The process of generating sentences using a transformer decoder begins with the conversion of initial token sequences \mathbf{t} into word embeddings, represented as $\mathbf{T}_{\text{embed}}$. This embedding transformation is defined as:

$$\mathbf{T}_{\text{embed}} = E_{\text{embed}}(\mathbf{t}) + E_{\text{pos}}, \quad (9)$$

where $E_{\text{embed}}(\mathbf{t})$ represents the token embeddings and E_{pos} is the positional encoding, which captures the sequential order of the tokens. These embeddings serve as the initial input to the transformer decoder as shown in Figure 4.

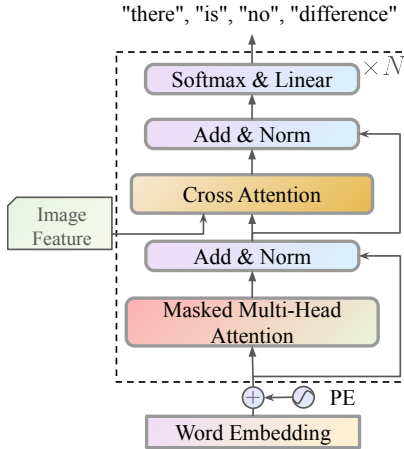


Fig. 4. The diagram illustrates the algorithmic workflow of the transformer decoder, highlighting the key processes of embedding, masked multi-head attention, feed-forward computation, and autoregressive token generation.

The next step involves passing $\mathbf{T}_{\text{embed}}$ through the masked multi-head self-attention (MHA) mechanism. At the core of this operation lies the computation of attention heads, defined as:

$$\mathbf{Head}_l = \text{Attention}(\mathbf{T}_{\text{embed}}^{i-1} \mathbf{W}_l^Q, \mathbf{T}_{\text{embed}}^{i-1} \mathbf{W}_l^K, \mathbf{T}_{\text{embed}}^{i-1} \mathbf{W}_l^V), \quad (10)$$

where the attention function is expressed as:

$$\text{Attention}(\mathbf{Q}, \mathbf{K}, \mathbf{V}) = \text{Softmax}\left(\frac{\mathbf{Q}\mathbf{K}^\top}{\sqrt{d}}\right) \mathbf{V}. \quad (11)$$

Here, $\mathbf{W}_l^Q, \mathbf{W}_l^K$, and $\mathbf{W}_l^V \in \mathbb{R}^{d_{\text{embed}} \times d_{\text{embed}}/h}$ are trainable projection matrices for the l -th attention head, where h denotes the number of attention heads and d_{embed} represents the embedding dimension. The outputs from all attention heads are concatenated and linearly projected using $\mathbf{W}^O \in \mathbb{R}^{d_{\text{embed}} \times d_{\text{embed}}}$, yielding the result of the MHA layer:

$$\begin{aligned} \mathbf{T}_{\text{img}} &= \text{MHA}(\mathbf{T}_{\text{embed}}^{i-1}, \mathbf{T}_{\text{embed}}^{i-1}, \mathbf{T}_{\text{embed}}^{i-1}) \\ &= \text{Concat}(\mathbf{Head}_1, \dots, \mathbf{Head}_h) \cdot \mathbf{W}^O \end{aligned} \quad (12)$$

Following the MHA sub-layer, the output undergoes further processing through a feed-forward network (FFN). The final output of the decoder layer is obtained by incorporating the input embedding $\mathbf{T}_{\text{embed}}^{i-1}$ with the output of the FFN via residual connections:

$$\mathbf{T}_{\text{text}} = \text{FN}(\mathbf{T}_{\text{img}}) + \mathbf{T}_{\text{embed}}^{i-1}. \quad (13)$$

To generate captions, the decoder output is passed through a linear transformation layer followed by a softmax activation function. This step converts the embedding into probabilities over the vocabulary space, yielding the final caption:

$$\text{Caption}_T = \text{Softmax}(\text{LN}(\mathbf{T}_{\text{text}})) \quad (14)$$

where $\text{Caption}_T = [\hat{t}_1, \hat{t}_2, \dots, \hat{t}_n] \in \mathbb{R}^{n \times m}$. Here, n represents the length of the generated caption, m denotes the vocabulary size, and \hat{t}_i corresponds to the predicted probability distribution for the i -th word.

Autoregressive Caption Generation. During the validation and testing phases, an autoregressive strategy is employed for caption generation. The decoder begins with a special “START” token and iteratively predicts the next token by conditioning on the previously generated tokens and the encoder’s output features. At each step, logits are computed using a linear transformation, and probabilities are derived via softmax. This process continues until the “END” token is generated, marking the completion of the caption.

This approach allows the model to effectively integrate information from the input image and previously generated tokens, ensuring coherent and contextually relevant caption generation.

IV. EXPERIMENTAL

A. Datasets

The LEVIR_MCI dataset [19] is a large-scale benchmark designed for remote sensing image change captioning tasks. It comprises 10,077 pairs of bi-temporal remote sensing images, each with a spatial resolution of 0.5 meters per pixel and a size of 256×256 pixels. These image pairs are sourced from 20 distinct regions in Texas, USA, capturing various urban and suburban developments over time. Each image pair is annotated with five descriptive sentences detailing the changes observed between the two time points, resulting in a total of 50,385 change captions. This dataset facilitates the development and evaluation of models that generate natural language descriptions of changes in remote sensing imagery.

The WHU-CDC dataset is derived primarily from the WHU-CD [20] dataset and includes high-resolution (0.075 m) image

pairs with dimensions of $32,507 \times 15,354$ pixels. These images document the construction of buildings in the Christchurch region following the 6.3 magnitude earthquake in February 2011 in New Zealand. From this source, the WHU-CDC dataset [21] provides 7,434 image pairs, each resized to 256×256 pixels, and is accompanied by 37,170 sentences describing the changes. The sentences range in length from three to 24 words, with a total vocabulary size of 327 unique words.

The Dubai-CC dataset[22] focuses on urban development changes in Dubai, United Arab Emirates. It consists of bi-temporal satellite images captured by the Enhanced Thematic Mapper Plus (ETM+) sensor onboard Landsat 7, dated May 19, 2000, and June 16, 2010. The original images are divided into 500 tiles, each measuring 50×50 pixels. Each tile is annotated with five change descriptions, totaling 2,500 captions. The dataset is partitioned into training, validation, and testing sets, containing 300, 50, and 150 bi-temporal tiles, respectively. Dubai-CC serves as a valuable resource for studying change captioning in rapidly urbanizing environments.

B. Experimental Setup

1) *Evaluation Metrics*: In evaluating natural language generation tasks, several automatic metrics are commonly employed to assess the quality of generated text:

- BLEU (Bilingual Evaluation Understudy): Introduced by Papineni et al. [23], BLEU is a precision-based metric for evaluating machine translation quality. It calculates the overlap between n-grams of the candidate and reference translations, with n typically ranging from 1 to 4. The BLEU score is computed as:

$$\text{BLEU} = \text{BP} \times \exp\left(\sum_{n=1}^N w_n \log p_n\right) \quad (15)$$

where p_n is the precision of n-grams, w_n are positive weights summing to one (often uniform), and BP is the brevity penalty to penalize short translations:

$$\text{BP} = \begin{cases} 1 & \text{if } c > r \\ \exp(1 - \frac{r}{c}) & \text{if } c \leq r \end{cases} \quad (16)$$

Here, c is the length of the candidate translation, and r is the length of the reference translation.

- ROUGE-L (Recall-Oriented Understudy for Gisting Evaluation): Part of the ROUGE metric family introduced by Lin [24], ROUGE-L evaluates the quality of summaries by measuring the longest common subsequence (LCS) between the candidate and reference texts. The ROUGE-L score considers both precision and recall:

$$F_\beta = \frac{(1 + \beta^2) \times \text{Precision} \times \text{Recall}}{\text{Precision} + \beta^2 \times \text{Recall}} \quad (17)$$

where $\text{Precision} = \frac{\text{LCS}(X,Y)}{\text{length of } X}$, $\text{Recall} = \frac{\text{LCS}(X,Y)}{\text{length of } Y}$, and β is a parameter that determines the relative importance of precision and recall.

- METEOR (Metric for Evaluation of Translation with Explicit Ordering): Proposed by Banerjee and Lavie [25], METEOR evaluates translation quality by aligning

words in the candidate and reference translations using exact matches, stemming, and synonyms. It computes a harmonic mean of unigram precision and recall, giving higher weight to recall, and includes a penalty for fragmented matches:

$$\text{METEOR} = F_{\text{mean}} \times (1 - \text{Penalty}) \quad (18)$$

where $F_{\text{mean}} = \frac{10 \times \text{Precision} \times \text{Recall}}{\text{Recall} + 9 \times \text{Precision}}$ and $\text{Penalty} = 0.5 \times \left(\frac{\text{chunks}}{\text{matches}}\right)^3$.

- CIDEr-D (Consensus-based Image Description Evaluation): Introduced by Vedantam et al. [26], CIDEr-D is designed for evaluating image descriptions by measuring the consensus between a candidate description and a set of reference descriptions. CIDEr-D applies TF-IDF weighting to n-grams, emphasizing the importance of less frequent, informative n-grams:

$$\text{CIDEr-D} = \frac{1}{m} \sum_{i=1}^m \sum_{n=1}^N w_n \cdot \text{CIDEr}_n \quad (19)$$

where m is the number of reference sentences, w_n is the TF-IDF weight for n-grams, and CIDEr_n measures the similarity of n-grams between the candidate and reference descriptions.

2) *Experimental Details*: The deep learning methods presented in this study were implemented using the PyTorch framework and executed on NVIDIA 4090 GPUs equipped with 24 GB of memory. The training and evaluation processes followed carefully designed parameters. The Adam optimizer [27] was employed with an initial learning rate of $5e-5$, while momentum and weight decay were set to 0.99 and 0.0005, respectively. The training process was conducted over approximately 200 epochs with a batch size of 8, ensuring computational efficiency.

C. Quantitative Results

Table I summarizes the performance of the proposed Mask Approx Net and competing methods on the LEVIR-CC dataset across multiple evaluation metrics. Mask Approx Net achieves state-of-the-art results, consistently outperforming all baseline methods. Notably, Mask Approx Net achieves the highest scores on key metrics such as BLEU-4 (64.32), METEOR (39.91), ROUGE-L (75.67), and CIDEr-D (137.71), demonstrating its superior ability to generate accurate and semantically rich descriptions. Compared to strong baselines such as SEN, Sparse Focus, and ATTENTIVE, the proposed method shows consistent improvements, particularly in CIDEr-D and BLEU scores, which are critical for assessing semantic relevance and fluency.

Overall, the results highlight the robustness and effectiveness of Mask Approx Net in capturing detailed semantic and structural information for change captioning, establishing it as the new state-of-the-art on the LEVIR-CC dataset.

The experimental results on the WHU-CDC dataset, presented in Table II, highlight the competitive performance of our proposed Mask Approx Net across multiple evaluation metrics. Mask Approx Net achieves the highest scores for

TABLE I
COMPARISON OF METHODS' PERFORMANCE ON MULTIPLE EVALUATION METRICS ON LEVIR-CC DATASET

Method	Metrics						
	BLEU-1	BLEU-2	BLEU-3	BLEU-4	METEOR	ROUGE-L	CIDEr-D
Capt-Rep-Diff	72.90	61.98	53.62	47.41	34.47	65.64	110.57
Capt-Att	77.64	67.40	59.24	53.15	36.58	69.73	121.22
Capt-Dual-Att	79.51	70.57	63.23	57.46	36.56	70.69	124.42
DUDA	81.44	72.22	64.24	57.79	37.15	71.04	124.32
MCCFormers-S	82.16	72.95	65.42	59.41	38.26	72.10	128.34
MCCFormers-D	80.49	71.11	63.52	57.34	38.23	71.40	126.85
RSICCformer	84.11	75.40	68.01	61.93	38.79	73.02	131.40
ATTENTIVE-S	82.41	73.10	65.29	59.02	38.71	72.47	130.88
ATTENTIVE	85.14	76.91	69.86	64.09	39.83	74.62	135.41
Sparse Focus	84.56	75.87	68.64	62.87	39.93	74.69	137.05
SEN	85.10	77.05	70.01	64.09	39.59	74.57	136.02
DiffusionRSCC	-	-	-	60.90	37.80	71.50	125.60
Mask Approx Net(ours)	85.90	77.12	70.72	64.32	39.91	75.67	137.71

BLEU-1 (81.34), BLEU-2 (75.68), BLEU-3 (71.16), BLEU-4 (67.73), and METEOR (43.89), demonstrating its effectiveness in generating accurate and semantically meaningful descriptions. Compared to MCCFormers-S, which achieves the highest ROUGE-L (78.52) and CIDEr-D (147.09) scores, Mask Approx Net achieves slightly lower results in these metrics but offers a balanced improvement across all BLEU and METEOR scores. This suggests that our method excels in maintaining both precision and semantic relevance, particularly in n-gram-based evaluations.

The performance of Mask Approx Net also surpasses MCCFormers-D and RSICCformer across most metrics, showcasing its robustness and adaptability to the WHU-CDC dataset. These results underscore the strength of our method in handling the challenges of remote sensing image change captioning, achieving state-of-the-art performance in key metrics.

D. Qualitative Visualization

The qualitative results in Figure 5 demonstrate the effectiveness of the proposed model in capturing semantic changes within remote sensing images. For instance, in scenarios where “a ring of houses surrounds the square,” the model successfully predicts “many villas are built around the road,” indicating a reasonable interpretation of structural changes. The predicted captions effectively capture major transitions, such as the replacement of natural features with urban structures or the emergence of roads and buildings. The generated change maps further validate the model’s capacity to align spatial transformations with semantic interpretations, showcasing its potential for practical applications in change detection tasks. Overall, the generated change maps and captions reveal the model’s capability to produce contextually relevant and visually coherent descriptions.

E. Limitation and Future Work

For the first time, we applied the diffusion model approach to the task of remote sensing image change captioning. Through this study, we summarize the existing challenges

and future directions as follows: 1. The training time of diffusion models, as well as their slow convergence and inference speed during training, remains a fundamental issue. 2. As an application-oriented research field, remote sensing image processing will increasingly focus on the model’s size, generalization ability, and robustness. 3. The semantic and logical alignment between images and descriptive text remains a key focus for future research.

V. CONCLUSION

In this paper, we presented a novel approach to remote sensing image change captioning by integrating diffusion models into the change captioning process. Our method shifts the focus from traditional feature learning paradigms to a data distribution learning perspective, addressing the limitations of existing CNN-based techniques. By incorporating a multi-scale change captioning module and refining the output features through a diffusion model, we have shown significant improvements in the robustness and adaptability of change captioning across different datasets and real-world scenarios. Furthermore, the introduction of the frequency-guided complex filter module ensures that high-frequency noise is effectively managed during the diffusion process, thereby preserving model performance.

The experimental results on multiple remote sensing change captioning description datasets validate the effectiveness of our proposed method, demonstrating superior performance compared to existing approaches. Our framework not only improves captioning accuracy but also enhances interpretability, contributing to a more comprehensive understanding of changes in remote sensing imagery. Future work will explore further optimizations of the diffusion process and extend the applicability of our approach to other multimodal tasks in remote sensing, ensuring even broader impact and usability in real-world applications.

REFERENCES

- [1] G. Hoxha, S. Chouaf, F. Melgani, and Y. Smara, “Change captioning: A new paradigm for multitemporal remote

TABLE II
COMPARISON OF METHODS' PERFORMANCE ON MULTIPLE EVALUATION METRICS ON WHU-CDC DATASET

Method	Metrics						
	BLEU-1	BLEU-2	BLEU-3	BLEU-4	METEOR	ROUGE-L	CIDEr-D
MCCFormers-S	81.12	75.04	69.95	65.34	42.11	78.52	147.09
MCCFormers-D	73.29	67.88	64.03	60.96	39.69	73.67	134.92
RSICCformer	80.05	74.24	69.61	66.54	42.65	73.91	133.44
Mask Approx Net(ours)	81.34	75.68	71.16	67.73	43.89	75.41	135.31

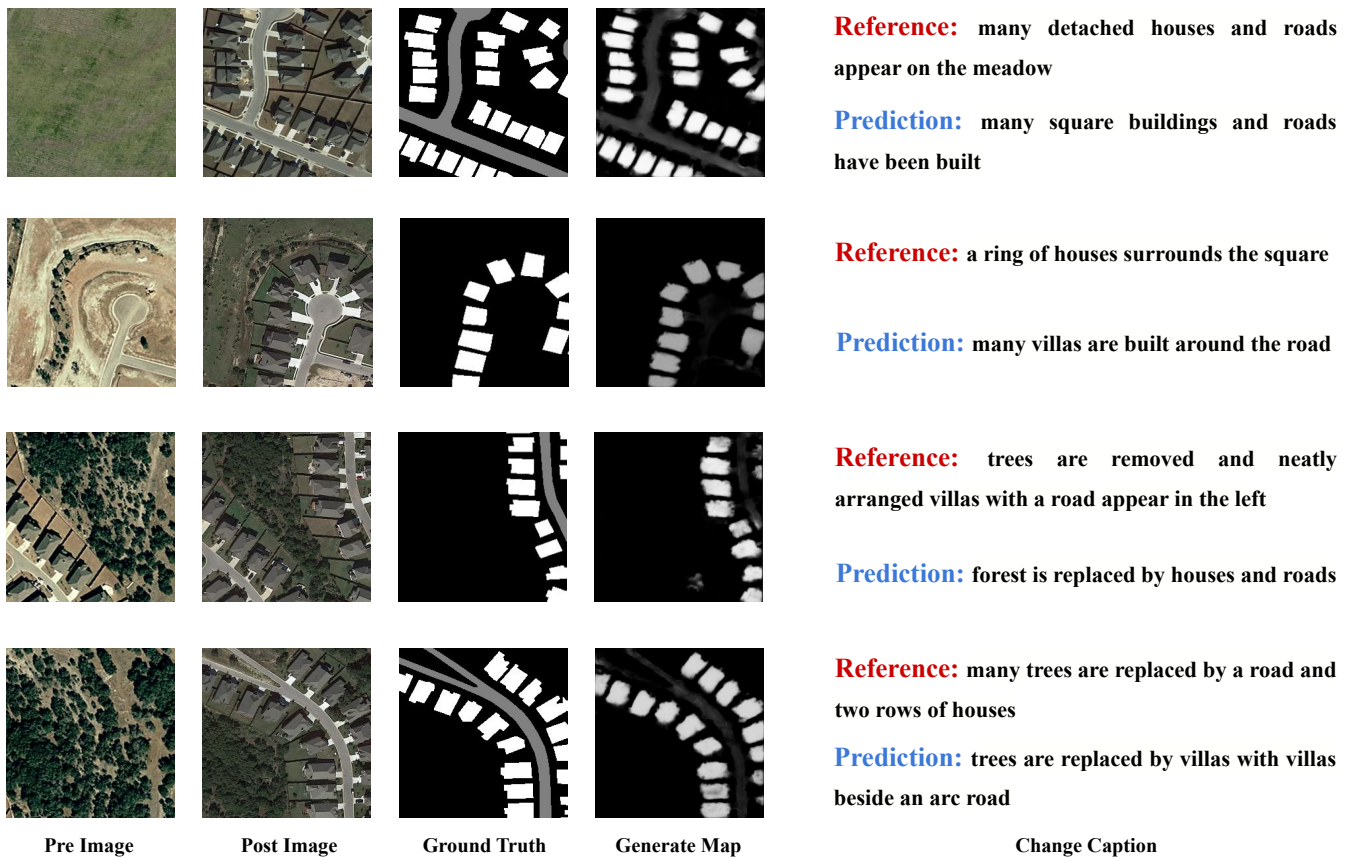


Fig. 5. Visualized image and captioning examples generated by Mask Approx Net on the LEVIR-MCI dataset

- sensing image analysis,” *IEEE Transactions on Geoscience and Remote Sensing*, vol. 60, pp. 1–14, 2022.
- [2] S. Chouaf, G. Hoxha, Y. Smara, and F. Melgani, “Captioning changes in bi-temporal remote sensing images,” in *2021 IEEE International Geoscience and Remote Sensing Symposium IGARSS*. IEEE, 2021, pp. 2891–2894.
- [3] A. Vaswani, N. Shazeer, N. Parmar, J. Uszkoreit, L. Jones, A. N. Gomez, L. u. Kaiser, and I. Polosukhin, “Attention is all you need,” in *Advances in Neural Information Processing Systems*, I. Guyon, U. V. Luxburg, S. Bengio, H. Wallach, R. Fergus, S. Vishwanathan, and R. Garnett, Eds., vol. 30. Curran Associates, Inc., 2017.
- [4] C. Liu, R. Zhao, H. Chen, Z. Zou, and Z. Shi, “Remote sensing image change captioning with dual-branch transformers: A new method and a large scale dataset,” *IEEE Transactions on Geoscience and Remote Sensing*, vol. 60, pp. 1–20, 2022.
- [5] C. Liu, J. Yang, Z. Qi, Z. Zou, and Z. Shi, “Progressive scale-aware network for remote sensing image change captioning,” in *IGARSS 2023-2023 IEEE International Geoscience and Remote Sensing Symposium*. IEEE, 2023, pp. 6668–6671.
- [6] C. Liu, R. Zhao, J. Chen, Z. Qi, Z. Zou, and Z. Shi, “A decoupling paradigm with prompt learning for remote sensing image change captioning,” *IEEE Transactions on Geoscience and Remote Sensing*, 2023.
- [7] S. Chang and P. Ghamisi, “Changes to captions: An attentive network for remote sensing change captioning,” *IEEE Transactions on Image Processing*, 2023.
- [8] D. Sun, Y. Bao, J. Liu, and X. Cao, “A lightweight sparse focus transformer for remote sensing image change cap-

- tioning,” *IEEE Journal of Selected Topics in Applied Earth Observations and Remote Sensing*, vol. 17, pp. 18 727–18 738, 2024.
- [9] X. Yu, Y. Li, and J. Ma, “Diffusion-rsc: Diffusion probabilistic model for change captioning in remote sensing images,” 2024. [Online]. Available: <https://arxiv.org/abs/2405.12875>
- [10] Q. Zhou, J. Gao, Y. Yuan, and Q. Wang, “Single-stream extractor network with contrastive pre-training for remote-sensing change captioning,” *IEEE Transactions on Geoscience and Remote Sensing*, vol. 62, pp. 1–14, 2024.
- [11] L. Qiu, X. Zhang, C. Gu, and S. Zhu, “A dual attentive generative adversarial network for remote sensing image change detection,” *arXiv preprint arXiv:2310.01876*, 2023.
- [12] J.-J. Wang, N. Dobigeon, M. Chabert, D.-C. Wang, T.-Z. Huang, and J. Huang, “Cd-gan: A robust fusion-based generative adversarial network for unsupervised remote sensing change detection with heterogeneous sensors,” *arXiv preprint arXiv:2203.00948*, 2022.
- [13] C. Ren, X. Wang, J. Gao, and H. Chen, “Unsupervised change detection in satellite images with generative adversarial network,” *arXiv preprint arXiv:2009.03630*, 2020.
- [14] W. G. C. Bandara, N. G. Nair, and V. M. Patel, “Ddpm-cd: Denoising diffusion probabilistic models as feature extractors for change detection,” *arXiv preprint arXiv:2206.11892*, 2022.
- [15] Y. Wen, X. Ma, X. Zhang, and M.-O. Pun, “Gcd-ddpm: A generative change detection model based on difference-feature guided ddpm,” *arXiv preprint arXiv:2306.03424*, 2023.
- [16] J. Wu, R. Fu, H. Fang, Y. Zhang, Y. Yang, H. Xiong, H. Liu, and Y. Xu, “Medsegdiff: Medical image segmentation with diffusion probabilistic model,” *arXiv preprint arXiv:2211.00611*, 2022.
- [17] W. Zhang, M. Li, J. Chen, Y. Zhou, and X. Wang, “A graph attention-guided diffusion model for liver vessel segmentation,” *Medical Image Analysis*, vol. 78, p. 102375, 2023.
- [18] W. G. C. Bandara and V. M. Patel, “Revisiting consistency regularization for semi-supervised change detection in remote sensing images,” 2022.
- [19] C. Liu, K. Chen, H. Zhang, Z. Qi, Z. Zou, and Z. Shi, “Change-agent: Toward interactive comprehensive remote sensing change interpretation and analysis,” *IEEE Transactions on Geoscience and Remote Sensing*, vol. 62, pp. 1–16, 2024.
- [20] S. Ji, S. Wei, and M. Lu, “Fully convolutional networks for multisource building extraction from an open aerial and satellite imagery data set,” *IEEE Transactions on Geoscience and Remote Sensing*, vol. 57, no. 1, pp. 574–586, 2019.
- [21] J. Shi, M. Zhang, Y. Hou, R. Zhi, and J. Liu, “A multitask network and two large-scale datasets for change detection and captioning in remote sensing images,” *IEEE Transactions on Geoscience and Remote Sensing*, vol. 62, pp. 1–17, 2024.
- [22] G. Hoxha, S. Chouaf, F. Melgani, and Y. Smara, “Change captioning: A new paradigm for multitemporal remote sensing image analysis,” *IEEE Transactions on Geoscience and Remote Sensing*, vol. 60, pp. 1–14, 2022.
- [23] K. Papineni, S. Roukos, T. Ward, and W.-J. Zhu, “Bleu: a method for automatic evaluation of machine translation,” in *Proceedings of the 40th Annual Meeting of the Association for Computational Linguistics*. Association for Computational Linguistics, 2002, pp. 311–318.
- [24] C.-Y. Lin, “Rouge: A package for automatic evaluation of summaries,” in *Text Summarization Branches Out: Proceedings of the ACL-04 Workshop*. Association for Computational Linguistics, 2004, pp. 74–81.
- [25] S. Banerjee and A. Lavie, “Meteor: An automatic metric for mt evaluation with improved correlation with human judgments,” in *Proceedings of the ACL Workshop on Intrinsic and Extrinsic Evaluation Measures for Machine Translation and/or Summarization*. Association for Computational Linguistics, 2005, pp. 65–72.
- [26] R. Vedantam, C. L. Zitnick, and D. Parikh, “Cider: Consensus-based image description evaluation,” in *Proceedings of the IEEE Conference on Computer Vision and Pattern Recognition*. IEEE, 2015, pp. 4566–4575.
- [27] D. Kingma and J. Ba, “Adam: A method for stochastic optimization,” *arXiv preprint arXiv:1412.6980*, 2014.